Journal of Structural Geology, Vol. 11, No. 6, pp. 751 to 762, 1989
Printed in Great Britain

0191-8141/89 $03.00 + 0.00

Initiation of cataclastic flow in a mylonite zone

SIMON HANMER

Lithosphere and Canadian Shield Division, Geological Survey of Canada,
588 Booth Street, Ottawa, Ontario, Canada K1A 0E4

(*Received* 13 *September* 1988; *accepted in revised form* 28 *March* 1989)

Abstract—At the mylonite–cataclasite transition in the homogeneous quartzo-feldspathic mylonites of the Great Slave Lake shear zone, northwest Canadian Shield, arrays of distributed macroscopic fractures evolved into zones of cataclastic flow. Fracture arrays occupy elliptical areas (metres by 10s of centimetres) aligned in the mylonite foliation plane. Fracture segments rotated either forwards or backwards in response to deformation. Where fractures rotated backwards, they remained planar and cataclasite did not develop. In the case of forward-rotation, only the central part of each fracture rotated. The rotated fracture segments are notably shorter and more closely spaced (1–2 mm) than those which have not rotated and the fracture array has a sigmoidal geometry. Cataclasite developed by the further deformation of such sigmoidal, forward-rotated fracture arrays.

Back-rotated fractures were initially planar, regularly spaced (2–10+ cm) and oriented at 70° to the mylonite foliation; they correspond to extensional faults. Forward-rotated fractures were initially planar, regularly spaced (2 cm) and oriented perpendicular to the mylonite foliation; they do not correspond to classical arrays of extensional or contractional faults. Both the initial orientation of the fractures and their subsequent rotational behaviour were constrained by the ability/inability of the wallrock to extend and by the ability/inability of the fractures to dilate.

Within the forward-rotated fracture arrays, cataclasite was produced after the rotated fracture segments had locked. It is proposed that a second perpendicular fracture set cut the earlier sigmoidal fractures resulting in stubby fragments of mylonite. The angular fragments acted as stress raisers within the otherwise homogeneous mylonite. This allowed the transition from distributed macroscopic fracture to impingement-induced localized microfracture and reduction of the fragment size with further strain. When a sufficient volume of interconnected fine material had formed, significant displacements could be accommodated by cataclastic flow, leading eventually to the development of thick (1–100s m) zones of cataclasite.

Models of cataclasis developed for porous and carbonate media predict initial grain-scale micro-fracture, slip and fragment rotation leading to frictional wear. The observations made in the Great Slave Lake shear zone suggest that such models may not be directly applicable to the initiation of cataclastic flow developed within non-porous, homogeneous, quartzo-feldspathic mylonite belts in crustal-scale fault zones, at the elevated confining pressures typical of the transition from the plastic to the brittle deformation regimes.

INTRODUCTION

AMBIENT conditions and physical properties, such as confining pressure, porosity, material continuity and wallrock stiffness are extremely important in determining the scale at which deformation processes operate and the sequence of structural development which leads to the initiation of cataclastic flow in continental-scale fault zones. The study of the development of natural cataclastic fault zones can shed light on the nature and role of such variables during natural deformation. It can also point to appropriate refinements of the design of laboratory experiments intended to simulate and quantify the transition to cataclastic flow in fault zones.

Cataclasis is essentially a process of distributed fracture and rotation (however, see Stel 1981, Chester *et al.* 1985). A basic requirement for cataclastic flow in porous media is the stabilization of fracture propagation by hardening (Blenkinsop & Rutter 1986). In porous media, work hardening may be induced by the collapse of pore spaces at moderate strains (Hirth & Tullis 1987, 1988), whereas in non-porous materials, hardening may be induced by increasing confining pressure (Byerlee 1968; however, see Hirth & Tullis 1986). Therefore, in order to successfully simulate initiation of a particular type of natural cataclastic flow in the laboratory, the experimentalist must carefully consider the appropriate material properties of the specimen and the boundary conditions of the deformation (e.g. Hadizadeh & Rutter 1983).

Geological research on cataclastic flow has concentrated on simulated and natural porous protoliths (e.g. Borg *et al.* 1960, Engelder 1974, Jackson & Dunn 1974, Logan *et al.* 1979, House & Gray 1982, Hadizadeh & Rutter 1983, Blenkinsop & Rutter 1986, Hirth & Tullis 1987). Few studies have examined cataclastic flow in non-porous granitic rocks (e.g. Stesky 1977, Anderson *et al.* 1980, 1983) or quartzites (Hirth & Tullis 1986). Moreover, no studies have specifically examined the development of cataclasite from intact, non-porous mylonite protolith (Jackson & Dunn 1974). While the cited experimental work was undertaken on zones of cataclasite a few millimetres thick in cm-scale rock specimens, the development of thick cataclasite zones has only received theoretical consideration (Sibson 1986a, Scholz 1987). It is therefore appropriate to document the development of thick belts of cataclasite from non-porous mylonite in a natural fault zone, at confining-pressures typical of the 'brittle–plastic' transition (Rutter 1986, Scholz 1988).

This contribution describes the mylonite–cataclasite transition in the quartzo-feldspathic ultramylonites of

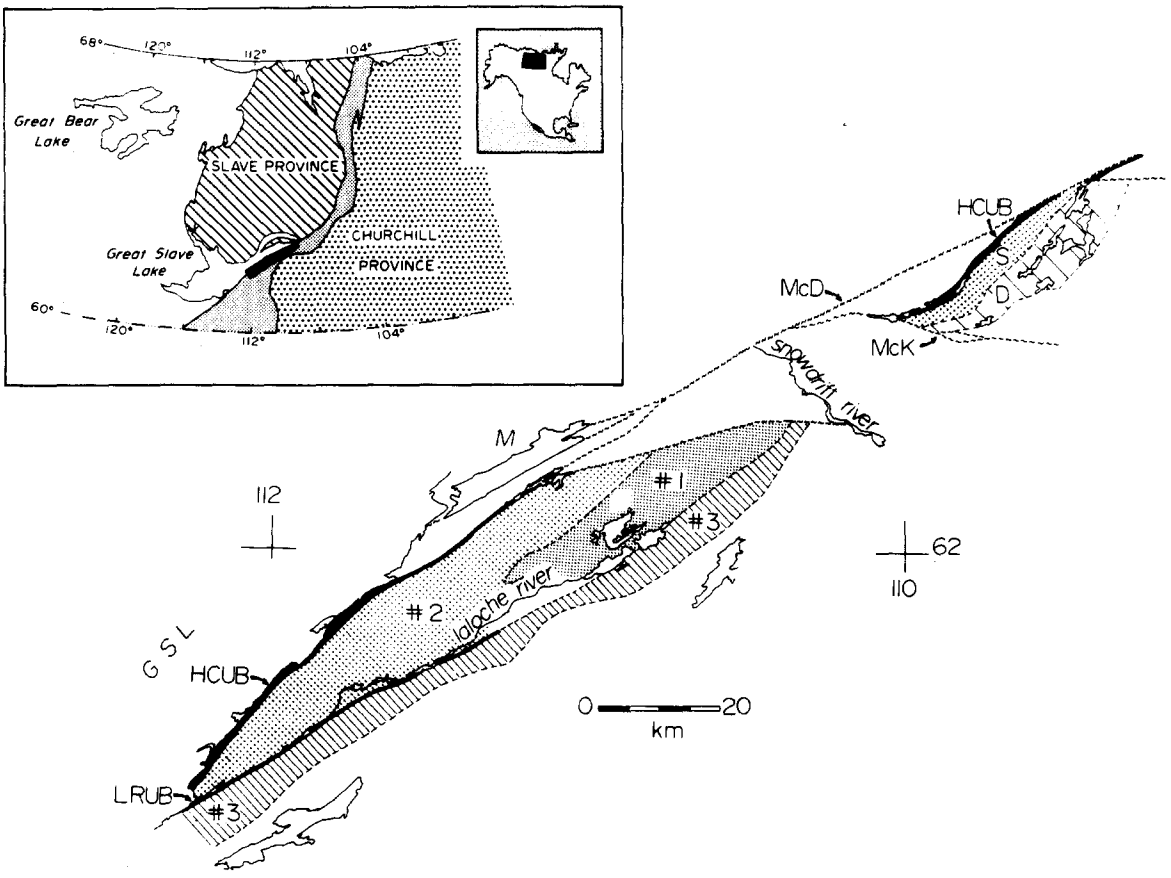

Fig. 1. Schematic map of the exposed section of the Great Slave Lake shear zone along the SE side of Great Slave Lake (GSL). In the dextral transcurrent SW segment, mylonite belts narrow with time and decreasing metamorphic grade; the belts are: No. 1 granulite, No. 2 upper-amphibolite, No. 3 lower-amphibolite, Hornby Channel (HCUB) and Laloche River (LRUB) lower-greenschist facies. The central segment (Snowdrift River area) is late-tectonic granite. The same relationship between metamorphic grade and width of the mylonite belts holds in the NE-segment, where the granulite facies Daisy Lakes mylonite belt (D) and the upper-amphibolite facies Schist Lakes mylonite belt (S) are significantly wider than the lower-greenschist HCUB. The McKee fault zone (McK) is marked by a greenschist mylonite zone up to 100 m wide. The McDonald Fault (McD) is a discrete non-mylonitic fault. The cataclasites are restricted to the greenschist-facies ultramylonite belts (LRUB, HCUB and McK). Inset is location of study area within the boundary zone between Slave and Churchill Provinces.

the Great Slave Lake shear zone, northwest Canadian Shield (Fig. 1) (Hanmer 1988a,b). Detectable distributed brittle deformation in the ultramylonites began at the macro-scale and evolved, without visible volume change (cf. Hadizadeh & Rutter 1983), into a micro-scale flow, rather than initiating directly as microscopic cataclastic flow. As will be seen below, the scale of the natural structure is such that the type of sequence described here would not normally be observed in experimental simulations since the laboratory specimens are too small. How does macroscopically spaced, distributed fracturing in a homogeneous material evolve into pervasive fracturing, fragment rotation and microscopic cataclastic flow, in the absence of macroscopic void space? Is this transition inherent in the fracture development or does it require a change of boundary conditions, such as a decrease in effective pressure? This paper examines, from a geological perspective, the influence of material properties, confining pressure and the kinematic and mechanical aspects of the deformation on the scale, initial orientation, spacing and rotational behaviour of fault arrays and the production of cataclasites.

The change of deformation regime from an essentially aseismic plastic lower crust to a seismogenic brittle upper crust has been equated with a 'brittle–ductile' transition (e.g. Sibson 1977; however, see Hobbs *et al.* 1986, Rutter 1986, Scholz 1988). From a micro-structural perspective, Sibson described this transition in terms of pressure-sensitive 'elastico-frictional' and temperature-sensitive 'quasi-plastic' regimes. However, from the perspective of rock mechanics and seismology, the transition could be represented entirely within the pressure-sensitive deformation field as the transition between slip on discrete faults and distributed flow by any process, such as microscopic cataclastic flow (Byerlee 1967, Logan 1979, Blenkinsop & Rutter 1986, Rutter 1986; however, see Hobbs *et al.* 1986). In this paper, rather than use the potentially equivocal 'brittle–ductile' terminology, I shall follow Rutter (1986) and describe the mylonite–cataclasite transition as 'plastic-to-brittle'. It will be shown that the transitional behaviour described here represents a change from temperature-sensitive crystal-plasticity to pressure-sensitive microscopic cataclastic flow, with a transient excursion into the field of distributed macroscopic faulting.

GREAT SLAVE LAKE SHEAR ZONE

The early Proterozoic Great Slave Lake shear zone is a crustal-scale, transcurrent mylonite zone up to 25 km wide, located at the contact between the Slave Craton and the Rae Province in the northwest Canadian Shield (Fig. 1) (Hanmer & Lucas 1985, Hanmer & Connelly 1986, Hanmer 1987, 1988a,b, Hanmer & Needham 1988). In outcrop it extends along the length of the East Arm of Great Slave Lake, continuing southwestwards under the Phanerozoic cover to the Rocky Mountain thrust belt (Hoffman 1987). In the present contribution, Great Slave Lake shear zone refers only to the section at outcrop.

In its southwestern segment, the Great Slave Lake shear zone comprises a bundle of five dextral, strike-slip mylonite belts, derived at the expense of a predominantly megacrystic granite protolith (Hanmer & Connelly 1986). Each belt is metamorphically monotonous; there are no metamorphic isograds preserved. Cross-cutting, transposition and reworking relationships observed in the field demonstrate that metamorphic pressure and temperature (granulite to lower-greenschist facies) and mylonite belt width decrease with time (Fig. 1) (Hanmer 1988a). Although kinematically more complex, the northeastern segment of the shear zone shows similar relationships among age, metamorphic grade and width of the mylonite belts (Hanmer & Needham 1988). The preservation of discrete belts of mylonite indicates that the decrease in shear zone width occurred step-wise with decay in strain rate in once-active volumes of the shear zone. These were then abandoned and occur now as higher grade, older mylonite belts. The narrowing of the mylonite belts with time reflects regional uplift and cooling, thermally induced stiffening of the wallrocks and, consequently, an increasing tendency to concentrate deformation within a narrow, mechanically strain-softened corridor. A more detailed account and discussion of the relationship of the mylonite belt width to pressure and temperature is given elsewhere (Hanmer 1988a). Subsequently, laterally continuous belts of cataclasite and penetrative, low-dilation breccia developed, up to 500 m wide, confined to the earlier formed lower-greenschist facies ultramylonite belts (Fig. 1). Their development represents continued cooling and depressurization of the shear zone (Hanmer 1988a).

The brittle whole-rock behaviour of two types of mylonite will be examined below; that of compositionally homogeneous ultramylonite formed at lower-greenschist facies (LRUB and HCUB, Fig. 1) and that of layered mylonite formed at lower-amphibolite facies (belt No. 3, Fig. 1). Cataclasite developed in the former, but not in the latter. The onset of brittle behaviour in the layered mylonites occurred in the quartz-poor layers, while the more quartzo-feldspathic layers were still warm enough to be capable of crystal–plastic flow. It pre-dates the behavioural transition in the younger, colder ultramylonites. Nevertheless, it is pertinent to this study because it allows comparison with a control case where some of the boundary conditions applying to the deformation of the ultramylonite protolith were relaxed.

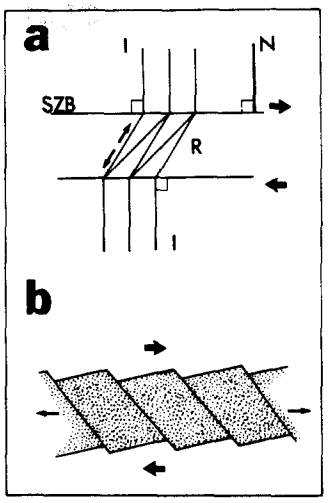

Fig. 2. Schematic representations of fracture arrays in homogeneous ultramylonites (a) and in layered mylonites (b). (a) Note the tapered, fault-bound sub-lithons developed within the forward-rotated rock-lithons to accommodate extension of the rock-lithons in homogeneous ultramylonites. The fractures are initiated orthogonal to the principal shear plane. (b) Note the preservation of the non-orthogonal angle made by the back-rotated shears with the principal shear plane in layered mylonites. The shaded layer is quartz-poor; the sense of shear along the principal shear plane is shown by thick arrows; extensional strain in rock-lithons or in the stiff quartz-poor layer due to fracture rotation is shown by small arrows; principal shear plane normal (N); rotated (R) and initial non-rotated (I) fracture segments; shear zone boundaries (SZB).

In the ultramylonites there are two expressions of brittle whole-rock behaviour. The one is represented by mappable belts of unfoliated cataclasites comprising an ultra-fine grained matrix surrounding variable proportions of mylonite rock fragments. The other is the development of arrays of distributed macroscopic faulting (Fig. 2a) in which marker horizons are barely disrupted (see Figs. 3a & b). The faults are distinctively curved. The common restriction of such faulting and the cataclasites to the lower-greenschist ultramylonite belts indicates that the fault arrays were precursors to the cataclasites. In contrast, brittle whole-rock behaviour in the amphibolite-facies mylonites gave rise to local arrays of planar faults (Fig. 2b), restricted to layers of relatively stiff calc-silicate rock or amphibolite set in a matrix of then still plastic granitic mylonite. This style of faulting did not develop into cataclasite. It is the intention of this study to compare the conditions of development for the two cases and to identify the factors controlling the development of cataclastic flow.

Protoliths

Homogeneous ultramylonites. Macroscopically, the quartzo-feldspathic ultramylonites are extremely fine grained, dark green and featureless or light grey/pink and very finely laminated. They are homogeneous up to the outcrop scale and shatter under the geological

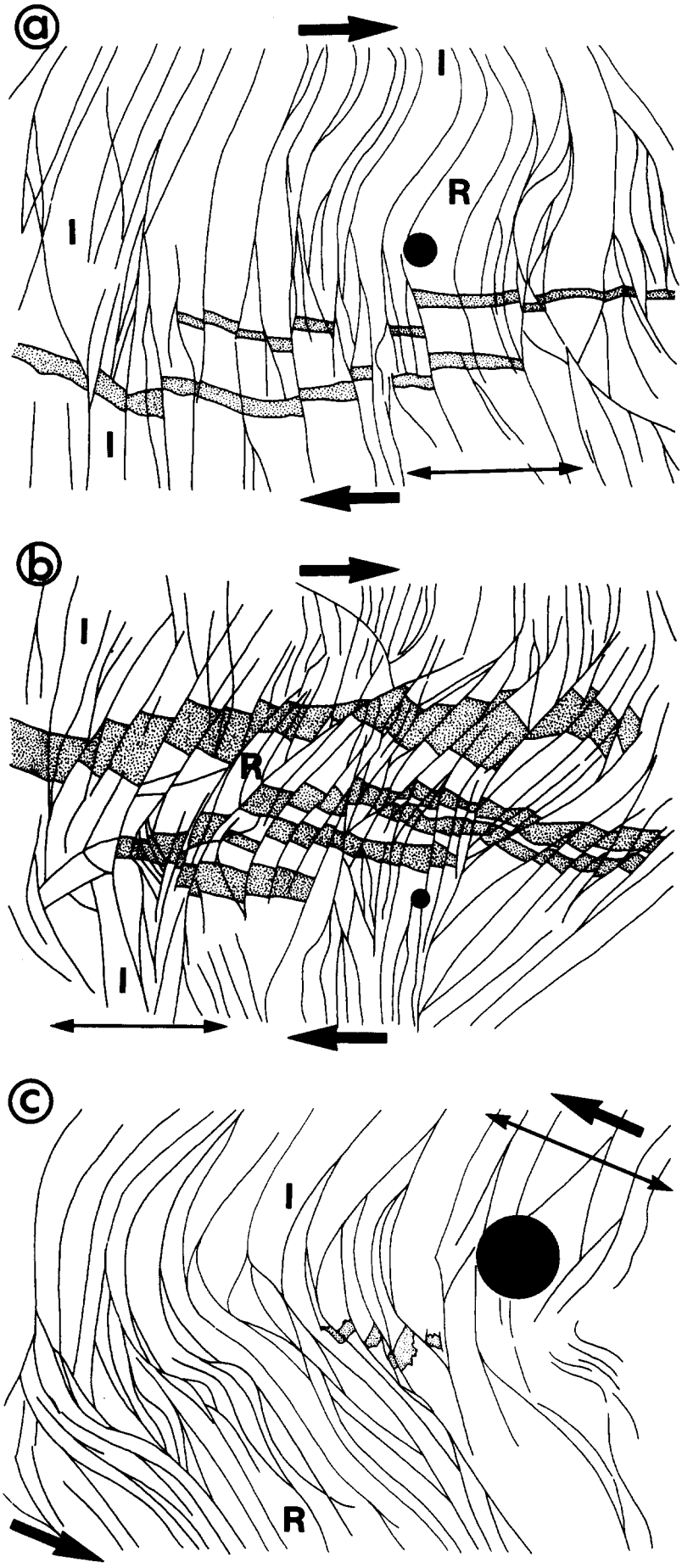

Fig. 3.

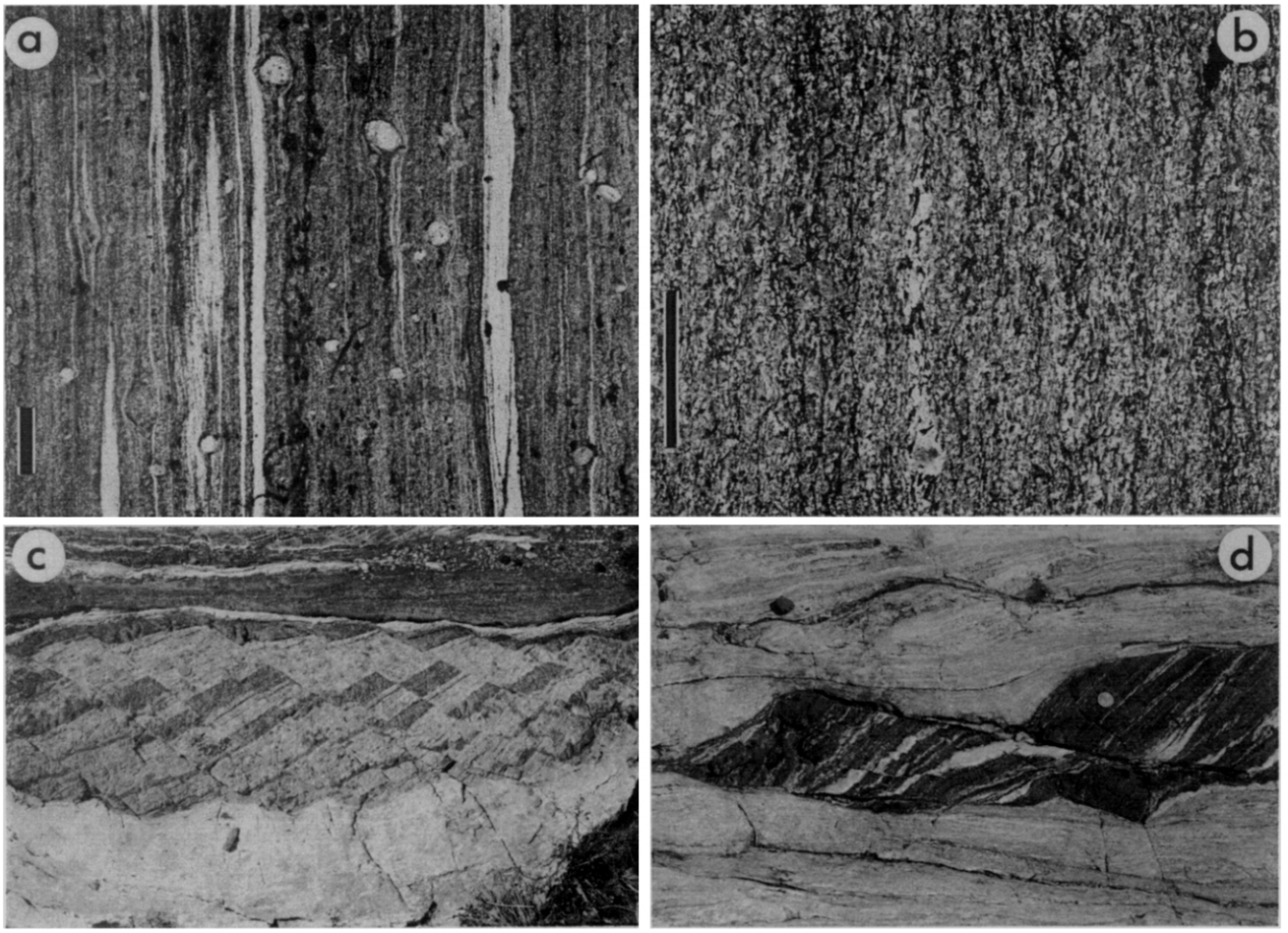

Fig. 4. (a & b) Microscopic aspects of mylonites prior to brittle deformation in the Great Slave Lake shear zone. Scale bars are 1 mm. (a) Ultramylonite formed at lower-greenschist facies, derived from amphibolite-facies mylonites. Note quartz ribbons (thin white streaks) set in ultrafine phyllosilicate matrix (dark grey). Thicker white bands are polycrystalline quartz. Note that there are very few feldspar porphyroclasts. (b) Ultramylonite formed at lower-amphibolite facies derived from a megacrystic granite protolith. Compared to (a), this rock shows poor quartz ribbon development (not shown), relatively coarser grain size in both quartz and feldspar and dispersed, aligned, subhedral biotite laths (dark). (c & d) Fracture arrays in layered mylonites in the Great Slave Lake shear zone. Fractures occur in quartz-poor layers which lie parallel to mylonite foliation, bounded on either side by plastic granitic mylonite capable of extensional shear flow. All show dextral bulk shear sense, not necessarily deduced from photos. The principal shear plane is parallel to the long dimension of each photograph and marked by the layering prior to block rotation. Scale coin is 23 mm in diameter. (c) Array of regularly spaced straight fractures in banded calc-silicate rock (centre) which initially made an angle of 70° with the principal shear plane. The initial angle is still preserved after back-rotation of the intervening rock-lithons and the rotated faults are still planar. (d) Extreme back-rotation of regularly spaced, straight fractures in banded amphibolite (dark). Fractures initially made an angle of 70° with the principal shear plane. Note plastic flow of bounding granitic mylonite (light) which accommodated the rotation of the stiff amphibolite slabs. Note also the cm-scale minor faults showing only minor slip within the left-hand back-rotated large lithon.

Fig. 3. Line drawings of arrays of fractures in homogeneous quartzo-feldspathic ultramylonites, observed on horizontal planes in the Great Slave Lake shear zone. Mylonitic foliation (long arrows) and fractures are oriented sub-perpendicular to page. Non-rotated (I) and rotated (R) fracture segments are indicated. Shear zone boundaries are irregular, but generally make a high angle with the non-rotated fracture segments. Bulk shear sense is indicated by thick arrows. Scales are 23 mm in diameter. (a) Fracture array with non-rotated (top and left) and forward-rotated fault segments (right). Note the regular spacing of the fractures, the increase in fracture density in the region of the bend and the laterally discontinuous sub-lithons (upper right). Non-rotated fracture segments bound parallel-sided rock-lithons (lower left). Offsets of veins (shaded) indicate some component of slip perpendicular to the plane of observation. (b) As (a), with forward-rotated fracture segments (centre) bounded above and below by non-rotated fracture segments. Note the regular fracture spacing and conservation of the perpendicular relationship between fractures and mylonite banding (spotted) in the rotated rock-lithons. (c) Non-rotated (above) and forward-rotated (below) fracture segments in a rare example of a sinistral fracture array. Again note the regular fracture spacing and the increase in fracture density in the rotated segments. A small quartz-filled vein (shaded) has opened across the length of several rock-lithons, but has subsequently been offset by new fractures bounding laterally discontinuous sub-lithons. The structures in (a–c) are strongly reminiscent of arrays described by Martel *et al.* (1988).

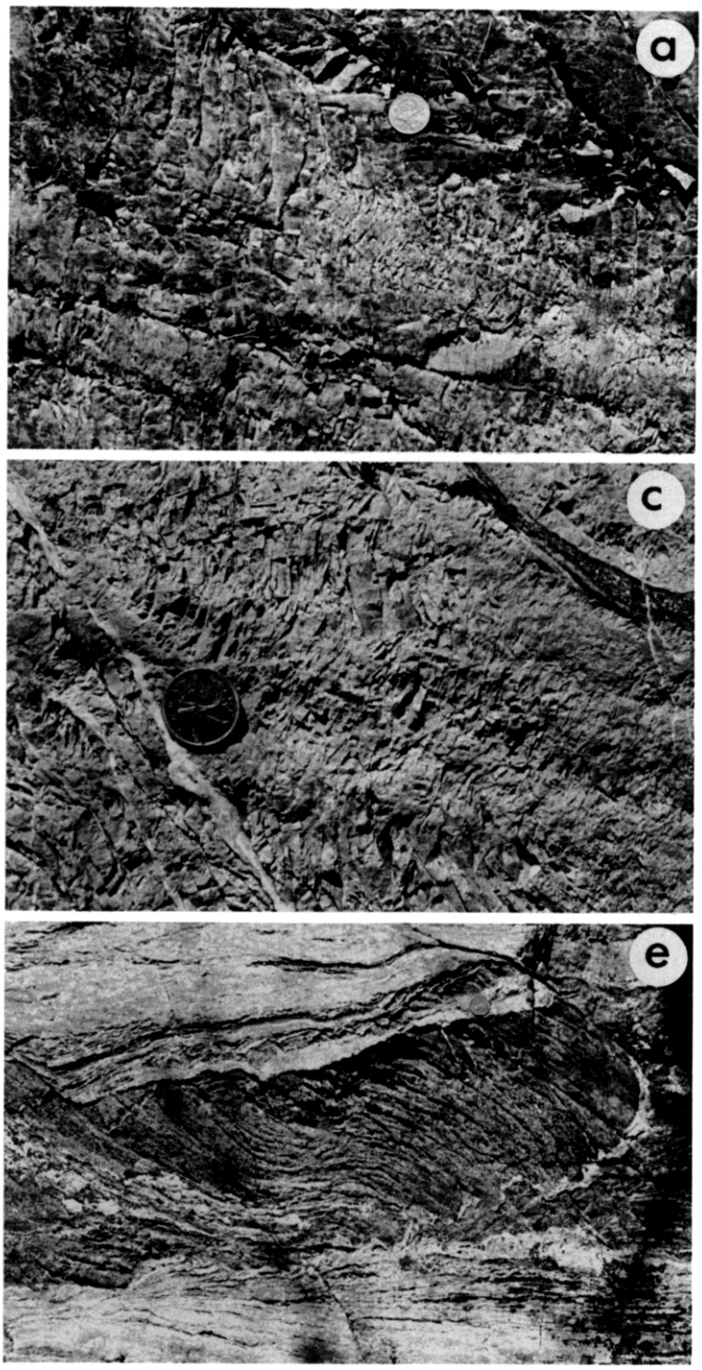

Fig. 5. (a–d) Details of deformed fracture arrays in homogeneous quartzo-feldspathic ultramylonites of the Great Slave Lake shear zone. The bulk shear sense indicated (thick arrows) was not deduced from structures in the figures. Long arrows are parallel to mylonite foliation trace. Non-rotated (I) and rotated (R) fracture segments are indicated. Scale coin is 23 mm in diameter. (a & b) Photograph and line drawing showing remarkably regular fracture spacing and relationship of spacing to forward-rotation of fracture segments. Compare the centre and lower right with the left and upper sides of the field of view. Note the absence of macroscopic dilation. (c & d) Photograph and line drawing of the interior part of a zone of complexly bent fracture segments. Note the close spacing of the fractures and the absence of macroscopic dilation, except for the post-rotation pseudotachylite vein (upper right) and later cross-cutting quartz veins (spotted). (e & f) Photograph and line drawing of back-rotation of regularly spaced, straight fractures in amphibolite (dark in photograph) in layered mylonite. Fractures initially made an angle of 70° with the principal shear plane. Plastic flow of bounding granitic mylonite (light in e) accommodated the rotation of the stiff amphibolite slabs. Note the local bending of the back-rotated fractures (centre) and the accompanying increase in fracture density in the rotated segment.

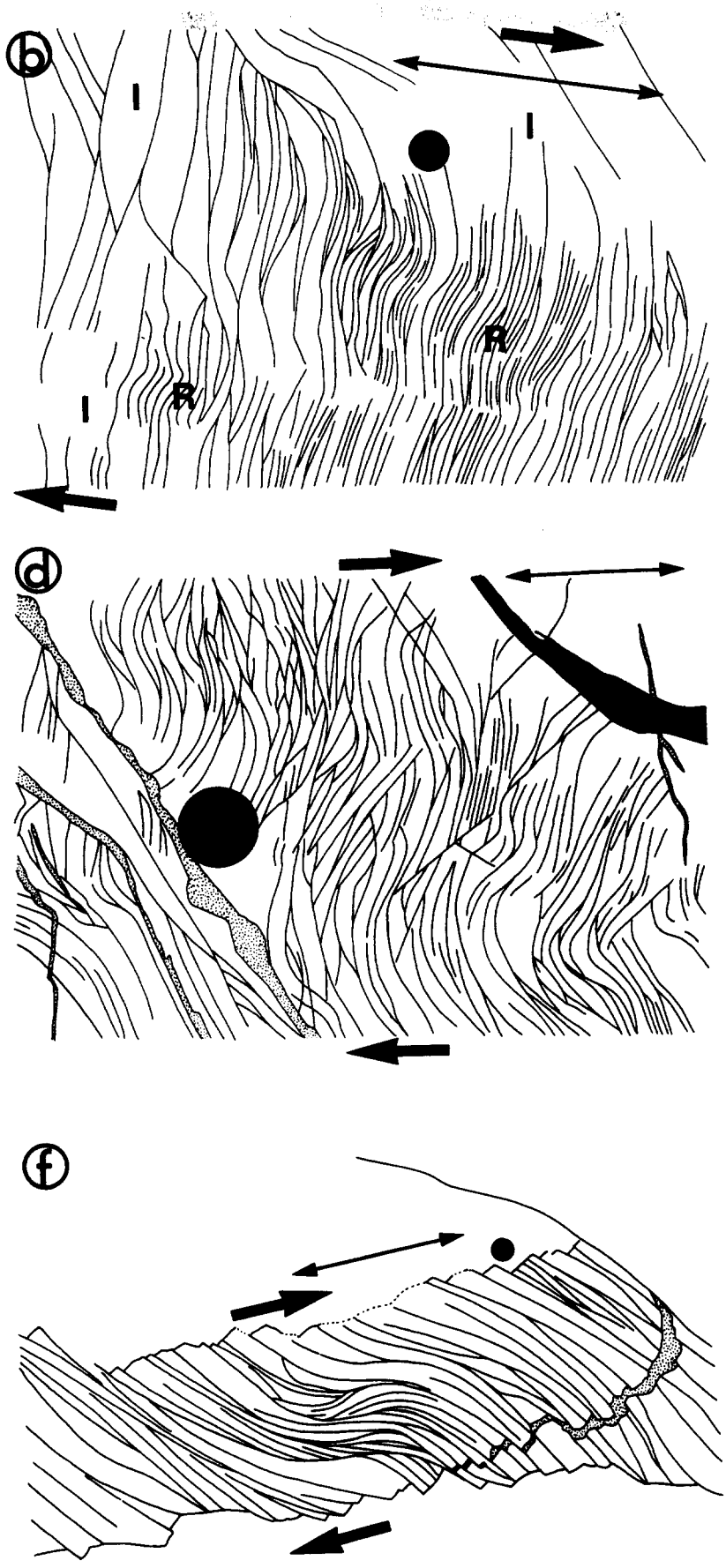

Fig. 5. *continued*.

hammer. Microscopically, they are banded, on a millimetric scale, according to the proportion of fine white mica derived at the expense of original feldspar (Fig. 4a). The quartz-rich bands are made of very fine (5 μm), equant to mildly elongate, internally strained quartz and feldspar grains. Equally fine white mica and chlorite flakes, sometimes aligned at a low angle to the bulk mylonite foliation are evenly dispersed along the grain boundary network, throughout the quartz-rich aggregate. Few, well rounded, 500 μm diameter, feldspar porphyroclasts are widely scattered through the fine matrix.

Layered mylonites. In outcrop the layered mylonites comprise foliation-parallel, metre-thick layers of amphibolite and calc-silicate rock set in a matrix of granitic mylonite (see Fig. 4c). The quartz-poor bands often show finer-scale internal layering. The granitic component ranges from porphyroclast-rich ribbon mylonites to ultramylonites, the macroscopic aspects of which have been described elsewhere (Hanmer 1987). Microscopically, the quartz-poor compositions comprise an annealed aggregate of well dispersed phases (Hanmer 1984). Considering only the matrix component, the granitic mylonites may show a millimetre-scale banding according to the proportion of feldspar. The quartz-rich bands are made of equant, 30 μm diameter, unstrained quartz and feldspar grains with foliation-parallel euhedral biotite (±white mica) flakes evenly dispersed along the grain boundary network (Fig. 4b). Garnet–sillimanite–biotite–white mica–quartz–feldspar assemblages in associated pelitic lithologies show that the mylonitization occurred at lower- to middle-amphibolite facies conditions (Hanmer 1988a).

Fracture arrays

Throughout its active history, Great Slave Lake shear zone was a dextral strike-slip structure (Hanmer & Lucas 1985, Hanmer & Connelly 1986, Hanmer 1988a,b, Hanmer & Needham 1988). The shear plane was parallel to the plane of the pre-existing mylonitic foliation even in the brittle regime. Figures 3–5 illustrate the typical geometry of fracture arrays developed in homogeneous quartzo-feldspathic ultramylonites and layered mylonites. Field observations were made on smooth, glacially polished exposures. Line drawings were made from field photographs. All descriptions refer to the horizontal plane. All fractures are steeply dipping and all rotations were effected about steeply plunging axes. While in general the fault patterns imply a two-dimensional finite strain (Reches 1978), in some outcrops displacements of marker bands indicate a minor component of slip along the axis of fault rotation. Inability to control this slip vector on individual slip planes requires that descriptions of the fracture array geometries remain qualitative. The geometries of the fracture arrays in the two types of protolith are now described.

Homogeneous ultramylonites. Fracture arrays occupy elliptical areas, up to several metres by several 10s of centimetres, whose long axes are aligned in the ultramylonite foliation plane. The mylonite foliation, banding and foliation-parallel veins of the host rock can be used as markers to provide a convenient reference frame for describing the fractures and their rotations, since they initially lie parallel to the principal shear plane of the brittle deformation (Figs. 2 and 3a & b). By comparing the orientations of fractures and markers in different parts of the fracture arrays, it can be shown that the arrays contain both rotated and non-rotated fracture segments. Initial or non-rotated fractures are planar, mutually sub-parallel, regularly spaced and approximately perpendicular to the mylonite foliation. The spacing is of the order of 2 cm. The fractures are macroscopically sharp and clean with no fracture fill. The intervening rock-lithons are undisturbed and in material continuity with the intact ultramylonite wallrock outside the array (Figs. 3a & c). Rotated fracture segments are similar, except that they are notably shorter and more closely spaced than non-rotated ones. They are gently curved and tend to link longer fractures which can still be traced into non-rotated segments (Figs. 3a & c and 5a & b); in other words they divide the parallel-sided rock-lithons into tapered sub-lithons (Figs. 3c and 5c & d). The rotated fracture segments are evenly spaced at the scale of a few millimetres, the exact distance varying from place to place. As the fractures rotate clockwise they slip sinistrally (Figs. 3b). In a few examples the fractures rotate anticlockwise and slip dextrally (Fig. 3c). Using the mylonitic banding or foliation as a marker, it can be shown that the initial fracture/foliation angle is maintained during rotation (Fig. 3b). However, cross-fractures may develop in some lithons which dilate and fill with quartz (Fig. 3c). The cross-fractures are indicative of extension imposed on the rotating slabs of mylonite between the fractures.

Layered mylonites. Fracture arrays in the layered mylonites are geometrically simpler than those in the ultramylonites (Figs. 4c & d). Planar fractures, regularly spaced at 2–10 cm intervals, cut across the foliation in quartz-poor layers at about 70° (Fig. 2b), but do not extend into the intervening granitic mylonite layers. While the majority of arrays comprise dextral faults lying anticlockwise to the shear plane normal (Fig. 2), arrays of clockwise conjugates are not uncommon. Dextral slip on the faults is accompanied by anticlockwise rotation, and vice versa, resulting in extension of the faulted layer along the principal shear plane (Fig. 2b). While kinematically akin to Riedel (R_1 or R) shears, they make a significantly greater initial angle with the principal shear plane (Tchalenko 1970, Wilcox *et al.* 1973, Logan *et al.* 1979). In contrast to the ultramylonites, the entire length of the initial fracture rotates with respect to the principal shear plane, as marked by the mylonitic foliation and banding; hence the faults generally do not bend (Figs. 2 and 4c & d). A further point of distinction is the timing of the development of

wide- and close-spaced faults. In the layered mylonites the initial fractures tend to be relatively closely spaced. In some cases, with rotation, a second-order set of regularly, but widely, spaced faults develops from the first set and accommodates the bulk of the rotation of the intervening large lithons (Fig. 4d). These geometrical relationships are comparable with those induced experimentally by combined shear and shear-parallel extension (Harris & Cobbold 1985, Behrmann 1987).

The granitic mylonite bounding the quartz-poor faulted layers was capable of plastic flow and accommodated the offsetting of the lithological boundaries without brittle failure (Figs. 4c & d). The common occurrence in these rocks of asymmetrical pull-apart structures (Hanmer 1986) and asymmetrical extensional shears (e.g. Platt & Vissers 1980), in combination with a high degree of ductility, confirms that flow in the granitic mylonites was able to accommodate the shear-parallel extension of the quartz-poor faulted layers.

Cataclasites

The cataclasites form deceptively simple looking, homogeneous exposures which, when etched by weathering, have a rubbly, granular to fragmental appearance. Where initial colours are preserved, light coloured, angular clasts of fine grained mylonite stand out against a generally non-foliated, monotonous grey, fine-grained matrix. Using internal mylonitic foliation as a marker, the clasts are mutually misoriented. More often, clasts and matrix share the same dark green colour. Clast dimensions, and those of strands of cataclasite, range from millimetres to 10s of metres. The map-scale belts of cataclasites, 100s of metres in width, represent corridors of complexly anastomosing strands of cataclasite enclosing large misoriented blocks of ultramylonite protolith. Cataclasite is heterogeneously developed through the ultramylonite belts; sudden changes in width and deflection around very large mylonite 'islands' make the cataclasite belts difficult to map systematically. However, at the scale of the shear zone, the distribution of cataclasite coincides with that of the greenschist-facies Laloche River and Hornby Channel ultramylonite belts and McKee fault zone (Fig. 1).

DISCUSSION

This study of cataclasis in the Great Slave Lake shear zone raises three main points:

(1) The exclusive map-scale spatial relationship between cataclasite and the quartzo-feldspathic ultramylonites formed at lower-greenschist facies indicates a truly progressive transition in deformation behaviour at a time when the ultramylonite belts were the loci of the final stages of important plastic strain. Effective confining pressures during the initiation of brittle deformation would have corresponded to depths of 10–15 km (up to 500 MPa), depending on the thermal gradient and pore fluid pressure (e.g. Sibson 1977).

(2) In contrast to most published models of the development of cataclasis (see Introduction), *initial micro-fractures*, which presumably preceded the deformation described here (e.g. Paterson 1978, Kranz 1983), *evolved into arrays of discrete macroscopic fractures rather than into a cataclasite*. Furthermore, mylonitic rocks which fractured under boundary conditions that allowed slipping faults to remain planar did not develop into cataclasite, whereas those with arrays whose component fractures bent synthetically with the imposed bulk shear developed into thick belts of cataclasis.

(3) The initial orientation of macroscopic fractures does not correspond to the classical kinematically controlled arrays of extensional (e.g. Tchalenko 1970, Wilcox *et al.* 1973) or contractional (e.g. Gamond 1983) faults described in the literature.

Discussion of the formation of cataclasite will be facilitated by the following brief discussion of the controls on macroscopic fracture orientation.

Distributed macroscopic fracture

Classical extensional fault models (e.g. Tchalenko 1970, Wilcox *et al.* 1973) require synthetic slip on, and consequent back-rotation of, the faults. However, such faults can only occur if boundary conditions permit extension in the direction of the imposed bulk shear plane (Freund 1974, Garfunkel & Ron 1985), unless compensating contractional structures are also formed. Material continuity between the array volume and rigid, unfaulted wallrocks will tend to suppress such fractures. Alternatively, arrays of high-angle, inclined contractional faults (e.g. Tchalenko 1970, Mandl 1987), as well as low-angle contractional faults (e.g. Gamond 1983), will slip antithetically and rotate forwards only if dilation is permitted. Significant effective confining pressures will tend to suppress such faulting. All of the above fault models are essentially kinematically controlled.

The condition for classical extensional faulting clearly applies to the case of the layered mylonites, in which the general non-coaxial strain in the plastic quartzo-feldspathic wallrocks required that the calc-silicate and amphibolite layers must extend in order to maintain some degree of coherence across the compositional contacts. They do so by synthetic slip and back-rotation of faults which initially make a significantly higher angle with the bulk shear plane than is typical of Riedel R_1 faults (Logan *et al.* 1979; see also Hanmer 1982, Faugere & Brun 1984, Gaudemer & Tapponnier 1987). It is pertinent to point out that in the rocks described here, the material between the faults is relatively stiff and approximately isotropic during faulting, whereas classical Riedel R_1 faults making an angle of 30° with the principal shear plane are commonly formed in ductile, often anisotropic, fault gouge (e.g. Tchalenko 1970, Wilcox *et al.* 1973, Logan 1979, Logan *et al.* 1979, Rutter *et al.* 1986). By contrast, in the brittle ultramylonites, material continuity of the rock-lithons with unyielding wallrocks outside the fault arrays would tend to resist such extension. Furthermore, the inference that frac-

turing occurs at confining pressures typical of the plastic-to-brittle transition and the observed lack of significant dilation suggest that contractional mode faults were inhibited by lithostatic load. Under such conditions, initially orthogonal shear fractures inherent to the 'bookshelf' model (e.g. Mandl 1987), in which 'books' rotate forwards and slip antithetically with respect to the bulk imposed shear, are kinematically favoured. The kinematic efficiency of such a model may be further enhanced since both the minor dilation inherent in the rotation of rigid 'books' and the length changes parallel and perpendicular to the principal shear plane are minimized if the 'books' can extend as they rotate (see below).

The sigmoidal geometry of the fault arrays in the ultramylonites can be described as that of a shear zone within the fault array. The preservation of non-rotated fault segments at the margins of the array, still in their initial orientation with respect to the bulk shear plane, is required to avoid disruption of the boundaries of the faulted volume (Fig. 2a). The shear zone boundaries make greater angles with the external non-rotated fault segments than with the internal rotated segments, which is geometrically consistent with extension of the rotated rock-lithons. Indeed, suppression of dilation at the shear zone boundaries by the effective confining pressure would require that the rock-lithons extend as they rotate. This interpretation is compatible with well established models of slip-plane rotation (e.g. Ramsay 1967, pp. 440–456, Freund 1974). In the brittle regime, the extension of the lithons is simply accommodated by slip on new intra-lithon fractures sub-parallel to, and of the same slip-sense as, the initial rotating faults. As a result, the lithons are divided into regularly spaced, tapered sub-lithons (Figs. 2a, 3 and 5a–d). A similar relationship between 'kinks' and fault spacing has been described by Segall & Pollard (1983) and Martel *et al.* (1988) who suggested that the rotation of fault segments to form 'kinks' occurred where the faults were most closely spaced. On the contrary, I suggest that the initiation of new fractures occurred during rotation of the rock-lithons, in order to accommodate an extensional strain within the lithons by homogeneously distributed faults, the regular spacing of which may be a reflection of a condition of minimum slip on individual fractures. This proposal derives some support from the observation that, in those rare cases in the layered mylonites where variation in finite strain and fracture rotation lead to sigmoidal fracture geometries, the fracture spacing decreases with rotation, as in the case of the ultramylonites (Figs. 5e & f).

Slip surfaces may lock up as they rotate towards stiff orientations with respect to the principal stresses or strains (Ramsay 1967, pp. 440–456, Nur *et al.* 1986). Why do the arrays of forward-rotated faults in the ultramylonites tend to lock up (Figs. 2a, 3 and 5a–d) and evolve into cataclasites, while the back-rotated faults in the layered mylonites clearly show no such effects (Figs. 2b and 4c & d)?

Microfracture and cataclasis

In the Great Slave Lake shear zone, deformation evolved from distributed macroscopic fracture into cataclasite at very specific sites: within shear zones developed in fracture arrays in those belts of ultramylonite that were the last sites of deformation in the plastic regime. Cataclasite was produced after the distributed macroscopic faults had rotated and locked. The fundamental problem in the transition from distributed macroscopic faulting to microscopic cataclastic flow is the accommodation of dilation as fragments attempt to fracture and rotate. Since the ultramylonite contains few localized stress raisers, such as porphyroclasts, how does this change in the scale of fragment comminution occur?

Consider a given array of forward-rotated, minimally dilated faults which has locked-up. Imposition of further bulk strain and bending of the rock-lithons could induce transverse cracking (e.g. Peng & Johnson 1972). However, such fractures would induce a dilation for which there is no macroscopic evidence. Alternatively, further bulk strain under similar boundary conditions to those which prevailed at the onset of faulting, might lead to initiation of a new set of fractures, oriented at an high angle to the principal shear plane (Mandl 1987), depending on the effect of the anisotropy induced by the earlier sigmoidal fractures. Superposition of a second array of straight fractures on an earlier sigmoidal set would result in smaller, stubbier fault-bound blocks than the rock-lithons and sub-lithons of the first fault array. This geometry should be particularly well developed in the zones of strongest curvature of the first fault array. Although I have nowhere found this stage well preserved, it is reasonable to suggest that the result would be a coarse, minimally-dilated aggregate of interlocking, angular fragments. Accordingly, prior to microscopic cataclastic flow, the network of distributed macroscopic faults of the first and second arrays would cut across the ultramylonite foliation at a variety of angles. The point here is that the aggregate of rock fragments would now contain relatively stiff, angular volumes which can act as stress raisers and indentors which can impinge upon their neighbours. The anisotropy of elastic response in mylonitic rocks (Johnson & Wenk 1974, Chroston & Max 1988), especially in ultramylonites (Jones & Nur 1982, 1984), might tend to enhance the relative stiffness of certain fragments as a function of the angular relationship between the mylonitic foliation and the bounding fractures.

Impingement of the newly created stress raisers will locally augment the differential stress and permit a new phase of finer scale pervasive fracturing. That this stage is not well preserved suggests a sudden increase in the instability of the aggregates and of the rate of fragment comminution. As the size of fragments decreases, so the pressure sensitivity of their rotation will decrease (e.g. Logan 1979, Tullis & Yund 1987). When a sufficient volume of interconnected, fine-grained matrix has been generated, significant macroscopic displacements can be

accommodated by cataclastic flow. Since microscopic cataclastic flow would have been initiated pervasively throughout the volume of a given fracture array, bands of cataclasite 10s by 100s cm will rapidly develop and may coalesce to form belts of cataclasite up to several 100s of metres thick.

The foregoing idealized sequence of fracturing events can be short-circuited by the introduction of a pore-fluid pressure, thus reducing the effective confining pressure. Reduction of the effective pressure after initiation of microscopic cataclasis would greatly enhance particulate flow (Rutter 1972, Borradaile 1981). However, if significant pore-fluid pressure were generated during the earlier part of the fracturing history, slip would be favoured over fracture (Hubbert & Rubey 1959, Byerlee 1967, 1968, Paterson 1978, p. 179) and a through-going fault should result instead of a belt of cataclasite.

Frictional slip on discrete faults, responsible for major seismic shock activity, is often preceded by premonitory micro-seismic slip (Logan 1979, Sibson 1986b). The initiation of arrays of distributed macroscopic faults in volumes measuring metres by decimetres might contribute to the micro-seismic signal of a fault zone. If so, observations in the deeply excavated Great Slave Lake shear zone suggest that some micro-seismic activity may in fact be the precursor to aseismic cataclastic flow in quartzo-feldspathic mylonitic rocks.

CONCLUSIONS

(1) At the plastic-to-brittle transition in homogeneous quartzo-feldspathic mylonites of the Great Slave Lake shear zone, detectable cataclasis began at the macro-scale and evolved, without visible volume change into a micro-scale flow, rather than initiating directly as microscopic cataclastic flow. Macroscopically spaced, distributed fracturing evolved into pervasive fracturing, fragment rotation and microscopic cataclastic flow, without the creation of macroscopic void space.

(2) The exclusive association of cataclastic development with the youngest and coldest mylonites of the Great Slave Lake shear zone suggests that the mylonite–cataclasite transition occurred at confining pressures typical of the plastic-to-brittle transition.

(3) The nature of initial fractures and their subsequent slip/rotation behaviour are controlled by (a) the ability of the wallrock to extend in the shear direction and (b) the ability of the fracture array to dilate. Rigid wallrocks and significant confining pressures favour the formation and forward-rotation of orthogonal 'book-shelf' fracture arrays and inhibit classical extensional and contractional fracturing.

(4) Cataclasite only develops in mylonites in which the fractures in the arrays bend during forward-rotation. Mylonites fractured under conditions where fractures are able to rotate backwards and remain planar do not develop into cataclasite.

(5) Within forward-rotated fracture arrays, cataclasite is produced after the rotated fractures have locked. It is suggested that a second fracture set cuts the earlier sigmoidal fracture set, resulting in an aggregate of tightly interlocked stubby fragments of ultramylonite.

(6) The transition from distributed macroscopic fracture to microscopic cataclasis is controlled by the impingement of the fracture-bound fragments which act as stress raisers. When a sufficient volume of interconnected fine material has formed, significant macroscopic displacement can be accommodated by cataclastic flow.

(7) The regular spacing of fractures may reflect a condition of minimum slip on individual faults. Such a condition is perhaps a function of the cross-over of threshold stress magnitudes for fracture and frictional sliding at elevated confining pressures.

(8) Models of cataclasis developed for porous media and which predict initial grain-scale microfracture, slip and fragment rotation leading to frictional wear, may not be directly applicable to the initiation of cataclastic flow developed with non-porous, homogeneous, quartzo-feldspathic mylonite belts in crustal-scale fault zones, at the confining pressures typical of the plastic-to-brittle transition.

Acknowledgements—An early version of this manuscript benefited from the thoughtful and detailed reviews of Steve Lucas, Leo Nadeau, Jack Henderson and Dick Brown. Further important improvements stemmed from the careful, critical reviews of Ernie Rutter and an anonymous reviewer, and I thank them both. This is Geological Survey of Canada Contribution No. 31488.

REFERENCES

Anderson, J. L., Osborne, R. H. & Palmer, D. F. 1980. Petrogenesis of cataclastic rocks within the San Andreas fault zone of southern California, U.S.A. *Tectonophysics* **67**, 221–249.

Anderson, J. L., Osborne, R. H. & Palmer, D. F. 1983. Cataclastic rocks of the San Gabriel Fault—an expression of deformation at deeper crustal levels in the San Andreas Fault Zone. *Tectonophysics* **98**, 209–251.

Behrmann, J. H. 1987. A precautionary note on shear bands as kinematic indicators. *J. Struct. Geol.* **9**, 659–666.

Blenkinsop, T. G. & Rutter, E. H. 1986. Cataclastic deformation of quartzite in the Moine thrust zone. *J. Struct. Geol.* **8**, 669–681.

Borg, I., Friedman, M., Handin, J. & Higgs, D. V. 1960. Experimental deformation of St. Peter Sand: a study of cataclastic flow. In: *Rock Deformation* (edited by Griggs, D. & Handin, J.). *Mem. geol. Soc. Am.* **79**, 133–192.

Borradaile, G. J. 1981. Particulate flow of rock and the formation of cleavage. *Tectonophysics* **72**, 305–322.

Byerlee, J. D. 1967. Frictional characteristics of granite under high confining pressure. *J. geophys. Res.* **72**, 3639–3648.

Byerlee, J. D. 1968. Brittle–ductile transition in rocks. *J. geophys. Res.* **73**, 4741–4750.

Chester, F. M., Friedman, M. & Logan, J. M. 1985. Foliated cataclasites. *Tectonophysics* **111**, 139–146.

Chroston, P. N. & Max, M. 1988. Seismic anisotropy in mylonites: an example from the Mannin Thrust zone, southwest Connemara, Ireland. *Tectonophysics* **148**, 29–39.

Engelder, J. T. 1974. Cataclasis and the generation of fault gouge. *Bull. geol. Soc. Am.* **85**, 1515–1522.

Faugere, E. & Brun, J.-P. 1984. Modélisation expérimentale de la distension continentale. *C. R. hebd. Séanc. Acad. Sci., Paris* **299**, 365–370.

Freund, R. 1974. Kinematics of transform and transcurrent faults. *Tectonophysics* **21**, 93–134.

Gamond, J. F. 1983. Displacement features associated with fault

zones: a comparison between observed examples and experimental models. *J. Struct. Geol.* **5**, 33–45.
Garfunkel, Z. & Ron, H. 1985. Block rotation and deformation by strike-slip faults. 2. The properties of a type of macroscopic discontinuous deformation. *J. geophys. Res.* **90**, 8589–8602.
Gaudemer, Y. & Tapponnier, P. 1987. Ductile and brittle deformations in the northern Snake Range, Nevada. *J. Struct. Geol.* **9**, 159–180.
Hanmer, S. 1982. Vein arrays as kinematic indicators in kinked anisotropic materials. *J. Struct. Geol.* **4**, 151–160.
Hanmer, S. 1984. Strain-insensitive foliations in polymineralic rocks. *Can. J. Earth Sci.* **21**, 1410–1414.
Hanmer, S. 1986. Asymmetrical pull-aparts and foliation fish as kinematic indicators. *J. Struct. Geol.* **8**, 111–122.
Hanmer, S. 1987. Textural map-units in quartzofeldspathic mylonitic rocks. *Can. J. Earth Sci.* **24**, 2065–2073.
Hanmer, S. 1988a. Great Slave Lake shear zone, Canadian Shield: reconstructed vertical profile of a crustal-scale fault zone. *Tectonophysics* **149**, 245–264.
Hanmer, S. 1988b. Geology, Great Slave Lake shear zone; parts of Fort Resolution, Snowdrift and Fort Reliance map areas, District of Mackenzie, NWT. Geological Survey of Canada, Open File 1783; 1:100,000.
Hanmer, S. & Connelly, J. N. 1986. Mechanical role of the syntectonic Laloche Batholith in the Great Slave Lake Shear Zone, District of Mackenzie, NWT. Current Research. *Geol. Surv. Pap. Can.* **86-1B**, 811–826.
Hanmer, S. & Lucas, S. B. 1985. Anatomy of a ductile transcurrent shear: the Great Slave Lake Shear Zone, District of Mackenzie, NWT (preliminary report). *Geol. Surv. Pap. Can.* **85-1B**, 7–22.
Hanmer, S. & Needham, T. 1988. Great Slave Lake shear zone meets Thelon Tectonic Zone, District of Mackenzie, NWT. Current Research. *Geol. Surv. Pap. Can.* **88-1A**, 33–49.
Harris, L. B. & Cobbold, P. R. 1985. Development of conjugate shear bands during bulk simple shearing. *J. Struct. Geol.* **7**, 37–44.
Hadizadeh, J. & Rutter, E. H. 1983. The low temperature brittle–ductile transition in a quartzite and the occurrence of cataclastic flow in nature. *Geol. Rdsch.* **72**, 493–509.
Hirth, G. & Tullis, J. 1986. Cataclastic flow of dry non-porous quartzite. *Eos* **67**, 1186.
Hirth, G. & Tullis, J. 1987. The transient nature of cataclastic flow in porous quartzite. *Eos* **68**, 1464.
Hirth, G. & Tullis, J. 1988. The effect of porosity on the room temperature deformation of quartzite. *Eos* **69**, 1446.
Hobbs, B. E., Ord, A. & Teyssier, C. 1986. Earthquakes in the ductile regime? *Pure & Appl. Geophys.* **124**, 309–336.
Hoffman, P. F. 1987. Continental transform tectonics: Great Slave Lake shear zone (*ca* 1.9 Ga), northwest Canada. *Geology* **15**, 785–788.
House, W. M. & Gray, D. R. 1982. Cataclasites along the Saltville thrust, U.S.A., and their implications for thrust sheet emplacement. *J. Struct. Geol.* **4**, 257–289.
Hubbert, M. K. & Rubey, W. W. 1959. Role of fluid pressure in mechanics of overthrust faulting. *Bull. geol. Soc. Am.* **70**, 115–166.
Jackson, R. E. & Dunn, D. E. 1974. Experimental sliding friction and cataclasis of foliated rocks. *Int. J. Rock Mech. & Mining Sci.* **11**, 235–249.
Johnson, L. R. & Wenk, H. R. 1974. Anisotropy of physical properties in metamorphic rocks. *Tectonophysics* **23**, 79–98.
Jones, T. & Nur, A. 1982. Seismic velocity and anisotropy in mylonites and the reflectivity of deep crustal fault zones. *Geology* **10**, 260–263.
Jones, T. & Nur, A. 1984. The nature of seismic reflections from deep crustal fault zones. *J. geophys. Res.* **89**, 3153–3171.
Kranz, R. L. 1983. Microcracks in rocks: a review. *Tectonophysics* **100**, 449–480.
Logan, J. M. 1979. Brittle phenomena. *Rev. Geophys. Space Phys.* **17**, 1121–1132.
Logan, J. M., Friedman, M., Higgs, N. G., Dengo, C. & Shimamoto, T. 1979. Experimental studies of simulated gouge and their application to studies of natural fault zones. In: *Natural Earthquake Hazard Reduction Program, 8th Conference on Analysis of Actual Faults in Bedrock*, Menlo Park, California, 305–343.
Martel, S. J., Pollard, D. D. & Segall, P. 1988. Development of simple strike-slip fault zones, Mount Abbot quadrangle, Sierra Nevada, California. *Bull. geol. Soc. Am.* **100**, 1451–1465.
Mandl, G. 1987. Tectonic deformation by rotating parallel faults: the "bookshelf" mechanism. *Tectonophysics* **141**, 277–316.
Nur, A., Ron, H. & Scotti, O. 1986. Fault mechanics and the kinematics of block rotations. *Geology* **14**, 746–749.
Paterson, M. S. 1978. *Experimental Rock Deformation: The Brittle Field.* Springer-Verlag, New York.
Peng, S. & Johnson, A. M. 1972. Crack growth and faulting in cylindrical specimens of Chelmsford Granite. *Int. J. Rock Mech. & Mining Sci.* **9**, 37–86.
Platt, J. P. & Vissers, R. L. 1980. Extensional structures in anisotropic rocks. *J. Struct. Geol.* **2**, 397–410.
Ramsay, J. G. 1967. *Folding and Fracturing of Rocks.* McGraw-Hill, New York.
Reches, Z. 1978. Analysis of faulting in a three dimensional strain field. *Tectonophysics* **47**, 109–129.
Rutter, E. H. 1972. The influence of interstitial water on the rheological behaviour of calcite rocks. *Tectonophysics* **14**, 13–33.
Rutter, E. H. 1986. On the nomenclature of mode of failure transitions in rocks. *Tectonophysics* **122**, 381–387.
Rutter, E. H., Maddock, R. H., Hall, S. H. & White, S. H. 1986. Comparative microstructures of naturally and experimentally produced clay-bearing fault gouges. *Pure & Appl. Geophys.* **124**, 3–30.
Scholz, C. H. 1987. Wear and gouge formation in brittle faulting. *Geology* **15**, 493–495.
Scholz, C. 1988. The brittle-plastic transition and the depth of seismic faulting. *Geol. Rdsch.* **77**, 319–328.
Segall, P. & Pollard, D. D. 1983. Nucleation and growth of strike slip faults in granite. *J. geophys. Res.* **88**, 555–568.
Sibson, R. H. 1977. Fault rocks and fault mechanisms. *J. geol. Soc. Lond.* **133**, 191–213.
Sibson, R. H. 1986a. Brecciation processes in fault zones: Inferences from earthquake rupturing. *Pure & Appl. Geophys.* **124**, 159–175.
Sibson, R. H. 1986b. Earthquakes and rock deformation in crustal fault zones. *Ann. Rev. Earth & Planet. Sci.* **14**, 149–175.
Stel, H. 1981. Crystal growth in cataclasites: diagnostic microstructures and implications. *Tectonophysics* **78**, 585–600.
Stesky, R. M. 1977. Mechanisms of high temperature frictional sliding in Westerly granite. *Can. J. Earth Sci.* **15**, 361–375.
Tchalenko, J. S. 1970. Similarities between shear zones of different magnitudes. *Bull. geol. Soc. Am.* **81**, 1625–1640.
Tullis, J. & Yund, R. A. 1987. Transition from cataclastic flow to dislocation creep of feldspar: mechanisms and microstructures. *Geology* **15**, 606–609.
Wilcox, R. E., Harding, T. P. & Seely, D. R. 1973. Basic wrench tectonics. *Bull. Am. Ass. Petrol. Geol.* **57**, 74–96.